

# Sixth-order coincidence fractional Fourier transform implemented with partially coherent light

F. Wang · Y. Cai · Y. Ma

Received: 28 April 2009 / Revised version: 28 June 2009 / Published online: 25 July 2009  
© Springer-Verlag 2009

**Abstract** The sixth-order coincidence fractional Fourier transform (FRT) with incoherent and partially coherent light is introduced as an extension of the recently introduced fourth-order coincidence FRT. An optical system for implementing sixth-order coincidence FRT is designed. It is found that the visibility of the sixth-order coincidence FRT pattern of an object is always much higher than that of the fourth-order coincidence FRT pattern. The visibility is closely related to the transverse width and the transverse coherence length of the light source and also depends on the fractional order of the optical system.

**PACS** 42.25.Kb · 42.30.Kq

## 1 Introduction

During the past several decades, especially since Wolf first found that partially coherent light undergoes a spectral shift during its propagation in free space [1, 2], partially coherent light has extensively been investigated both in experiment and theory [3]. Many interesting phenomena due to the low coherence of light have been reported, such as a spectral switch of partially coherent light [4, 5], reduced pointing errors in atmosphere communication with partially coherent light [6], enhanced conversion efficiency for second-harmonic generation [7, 8] etc. Partially coherent light has

been widely applied in practice, such as for optical projection, laser scanning, improving the uniformity of the intensity distribution in inertial confinement fusion and for the reduction of noise in photography [8–11].

Partially coherent light is characterized by a second-order correlation function of the electric field [3]. A Gaussian Schell-model (GSM) source is a typical partially coherent light source, which emits partially coherent beam whose spectral density and spectral degree of coherence have Gaussian shapes [12–14]. By scattering a coherent laser beam from a rotating grounded glass, then transforming the spectral density distribution of the scattered light into a Gaussian profile with a Gaussian amplitude filter, a GSM beam can be generated [15, 16]. GSM beams can also be generated with specially synthesized rough surfaces, spatial light modulators and synthetic acousto-optic holograms (cf. [17]). Recently, much attention has been paid to electromagnetic (i.e., vectorial) GSM source [18–21].

The concept of the fractional Fourier transform (FRT) was firstly proposed by Namias in 1980 as a generalization of the conventional Fourier transform [22]. McBride and Kerr developed Namias's theory to a more rigorous form [23]. In 1993, Ozaktas, Mendlovic and Lohmann introduced the FRT into optics and designed optical systems to achieve FRT [24–26]. Since then, the FRT has been used widely in signal processing, optical image encryption and beam analysis [27–29] etc. The FRT optical system also provides a convenient way to control the properties, e.g., the intensity distribution, spectral degree of coherence, polarization and spectrum of coherent and partially coherent beams [30–36].

In 2005, Cai et al. introduced the concept of coincidence FRT and designed an optical system for implementing the coincidence FRT with incoherent light, partially coherent light and entangled photon pairs [37, 38] as an extension of

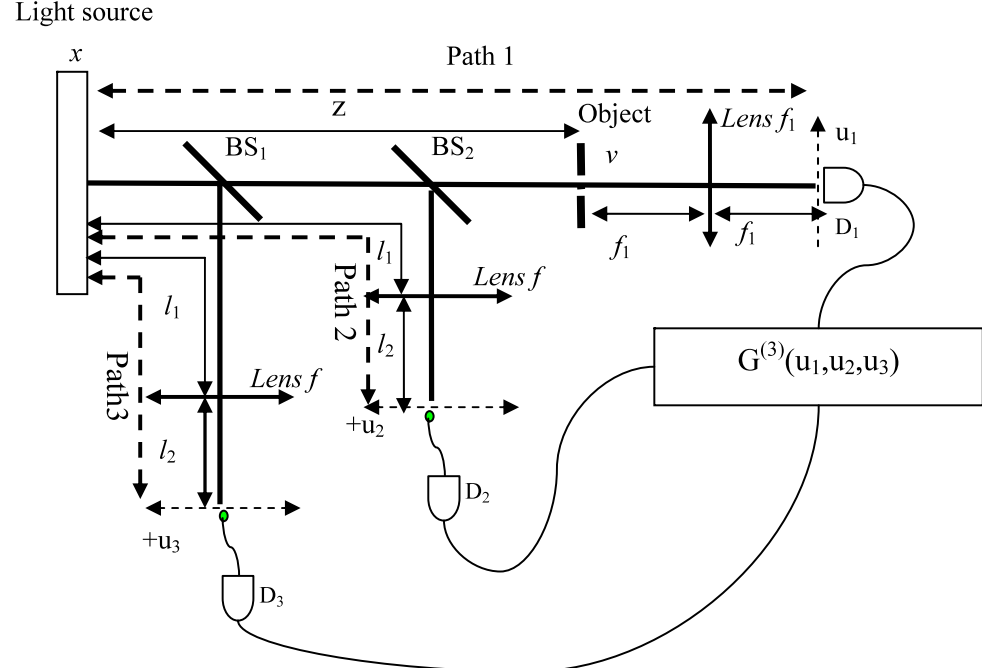
F. Wang · Y. Cai (✉)  
School of Physical Science and Technology, Soochow University,  
Suzhou 215006, China  
e-mail: [yangjian\\_cai@yahoo.com.cn](mailto:yangjian_cai@yahoo.com.cn)

Y. Ma  
Institute of Optics, Information and Photonics, University  
Erlangen-Nuremberg, Staudtstr. 7/B2, 91058 Erlangen, Germany

coincidence Fourier transform (also named ghost imaging and interference) [39–47]. Coincidence FRT is a method to obtain the FRT pattern of an object by measuring the coincidence counting rate (i.e., the fourth-order correlation) of two detected signals going through two different light paths, and the object is located in one light path [37, 38]. The coincidence subwavelength FRT was studied in [48]. The lensless optical implementation of the coincidence fractional Fourier transform was analyzed in [49]. Wang et al. successfully observed the coincidence FRT pattern of an object implemented with partially coherent light in experiment [50].

For the case of fourth-order coincidence FRT with entangled photon pairs, the visibility of the FRT pattern of an object is very high, but we know it is not cheap and easy to produce and control entangled photon pairs, which limits its application. For the case of fourth-order coincidence FRT with incoherent and partially coherent light, the visibility of the FRT pattern of an object is low because of the inevitable background noise as shown in [37] and [38], which also limits its application. Therefore it is interesting and valuable to propose a new method to enhance the visibility of the coincidence FRT pattern with classical light. In this paper, enlightened by the recently introduced higher-order coincidence Fourier transform (i.e., higher-order ghost imaging and interference) [51–54], we introduce the sixth-order coincidence FRT with incoherent and partially coherent light, and design an optical system for implementing this sixth-order coincidence FRT. Our results show that we can enhance the visibility of the coincidence FRT pattern of an object using our new method.

**Fig. 1** Optical system for implementing the sixth-order coincidence fractional Fourier transform with incoherent and partially coherent light



## 2 Theory

In this section, we introduce sixth-order coincidence fractional Fourier transform (FRT) implemented with incoherent and partially coherent light. The optical system for implementing sixth-order coincidence FRT with incoherent light is shown in Fig. 1. The light emitted from the source is firstly split into two beams by a beam splitter (BS<sub>1</sub>). The reflected beam propagates through path 3 to detector D<sub>3</sub>. The transmitted beam is split into two beams by a second beam splitter (BS<sub>2</sub>); then the two outgoing beams propagate through paths 1 and 2 to detector D<sub>1</sub> and D<sub>2</sub>, respectively. D<sub>1</sub>, D<sub>2</sub> and D<sub>3</sub> are single-photon detectors, D<sub>1</sub> is fixed at  $u_1 = 0$ , D<sub>2</sub> and D<sub>3</sub> are connected with single mode optical fibers whose tips are scanning on the transverse planes  $u_2$  and  $u_3$  separately. In path 1, there is an object with transmission function  $H(v)$  between the second beam splitter and D<sub>1</sub>, and a thin lens with focal length  $f_1$  exists between the object and D<sub>1</sub>. The distance from the object to the thin lens and the distance from the thin lens to D<sub>1</sub> both are  $f_1$ . In path 2, there is a thin lens with focal length  $f$  between the second beam splitter and D<sub>2</sub>, and the distance from the light source to the thin lens and the distance from the thin lens to D<sub>2</sub> are  $l_1$  and  $l_2$ , respectively. Path 3 is almost identical to path 2. The output signals from D<sub>1</sub>, D<sub>2</sub> and D<sub>3</sub> are then sent to an electronic coincidence circuit to measure the coincidence counting rate (i.e., the sixth-order correlation,  $G^{(3)}(u_1, u_2, u_3)$ ) of three detected signals.

Based on classical optical coherence theory and by use of the moment theorem, the sixth-order correlation function

of the classical incoherent or partially coherent light source can be expanded in terms of the second-order correlation function as follows [3]:

$$\begin{aligned} & \langle E_s^*(x'_1)E_s^*(x'_2)E_s^*(x'_3)E_s(x_1)E_s(x_2)E_s(x_3) \rangle \\ &= \langle E_s^*(x'_1)E_s(x_1) \rangle (\langle E_s^*(x'_2)E_s(x_3) \rangle \langle E_s^*(x'_3)E_s(x_2) \rangle \\ &+ \langle E_s^*(x'_2)E_s(x_2) \rangle \langle E_s^*(x'_3)E_s(x_3) \rangle) \\ &+ \langle E_s^*(x'_1)E_s(x_2) \rangle (\langle E_s^*(x'_2)E_s(x_1) \rangle \langle E_s^*(x'_3)E_s(x_3) \rangle \\ &+ \langle E_s^*(x'_2)E_s(x_3) \rangle \langle E_s^*(x'_3)E_s(x_1) \rangle) \\ &+ \langle E_s^*(x'_1)E_s(x_3) \rangle (\langle E_s^*(x'_2)E_s(x_2) \rangle \langle E_s^*(x'_3)E_s(x_1) \rangle \\ &+ \langle E_s^*(x'_2)E_s(x_1) \rangle \langle E_s^*(x'_3)E_s(x_2) \rangle), \end{aligned} \quad (1)$$

where  $E_s(x_i)$  ( $i = 1, 2, 3$ ) denotes the electric field of the light in the source plane, the asterisk denotes the complex conjugate and the angular brackets denote the ensemble average.  $\langle E_s^*(x_i)E_s(x_j) \rangle$  ( $i, j = 1, 2, 3$ ) denotes the second-order correlation function of the light in the source plane.

After propagating through the optical system as shown in Fig. 1, the second-order correlation function between two arbitrary detectors can be expressed as follows:

$$\begin{aligned} \langle E^*(u_i)E(u_j) \rangle &= \int_{-\infty}^{\infty} \int_{-\infty}^{\infty} \langle E_s^*(x_1)E_s(x_2) \rangle h_i^*(x_1, u_i) \\ &\times h_j(x_2, u_j) dx_1 dx_2, \end{aligned} \quad (2)$$

where  $E(u_i)$  ( $i = 1, 2, 3$ ) is the electrical field at the receiver detector.  $h_1(x, u_1)$ ,  $h_2(x, u_2)$  and  $h_3(x, u_3)$  are the response functions of the three optical paths in Fig. 1, respectively. By applying (1) and (2), we express the sixth-order correlation function  $G^{(3)}(u_1, u_2, u_3) = \langle E^*(u_1)E^*(u_2)E^*(u_3)E(u_1) \times E(u_2)E(u_3) \rangle$  (i.e., the sixth-order coincidence counting rate) of three detectors as follows:

$$\begin{aligned} G^{(3)}(u_1, u_2, u_3) &= \langle I_1(u_1) \rangle \langle I_2(u_2) \rangle \langle I_3(u_3) \rangle + \langle I_1(u_1) \rangle |\Gamma_{23}(u_2, u_3)|^2 \\ &+ \langle I_2(u_2) \rangle |\Gamma_{13}(u_1, u_3)|^2 + \langle I_3(u_3) \rangle |\Gamma_{12}(u_1, u_2)|^2 \\ &+ \Gamma_{12}(u_1, u_2)\Gamma_{23}(u_2, u_3)\Gamma_{31}(u_1, u_3) \\ &+ (\Gamma_{12}(u_1, u_2)\Gamma_{23}(u_2, u_3)\Gamma_{31}(u_1, u_3))^*, \end{aligned} \quad (3)$$

with

$$\begin{aligned} \langle I_i(u_i) \rangle &= \int_{-\infty}^{\infty} \int_{-\infty}^{\infty} \langle E_s^*(x_1)E_s(x_2) \rangle \\ &\times h_i^*(x_1, u_i)h_i(x_2, u_i) dx_1 dx_2, \quad i = 1, 2, 3, \end{aligned} \quad (4)$$

$$\begin{aligned} \Gamma_{ij}(u_i, u_j) &= \int_{-\infty}^{\infty} \int_{-\infty}^{\infty} \langle E_s^*(x_1)E_s(x_2) \rangle h_i^*(x_1, u_i) \\ &\times h_j(x_2, u_j) dx_1 dx_2, \quad i, j = 1, 2, 3 \end{aligned} \quad (5)$$

where  $\langle I_i(u_i) \rangle$  ( $i = 1, 2, 3$ ) is the average intensity distribution at the  $i$ -th detector.  $\Gamma_{ij}(u_i, u_j)$  ( $i, j = 1, 2, 3$ ) is the second-order correlation function between two different detectors  $D_i$  and  $D_j$ . Equations (4) and (5) are valid for the optical system under the condition of linear shift invariance and in the paraxial regime.

With the help of the matrix method [55], the response functions of the paths 1, 2 and 3 can be expressed as follows:

$$\begin{aligned} h_1(x, u_1) &= \left( -\frac{1}{\lambda^2 z f_1} \right)^{1/2} \\ &\times \int_{-\infty}^{\infty} H(v) \exp \left[ -\frac{i\pi}{\lambda z} (x^2 - 2xv + v^2) \right] \\ &\times \exp \left( \frac{2i\pi}{\lambda f_1} vu_1 \right) dv, \end{aligned} \quad (6)$$

$$h_2(x, u_2)$$

$$= \left( -\frac{i}{\lambda b_2} \right)^{1/2} \exp \left[ -\frac{i\pi}{\lambda b_2} (a_2 x^2 - 2xu_2 + d_2 u_2^2) \right], \quad (7)$$

$$h_3(x, u_3)$$

$$= \left( -\frac{i}{\lambda b_2} \right)^{1/2} \exp \left[ -\frac{i\pi}{\lambda b_2} (a_2 x^2 - 2xu_3 + d_2 u_3^2) \right], \quad (8)$$

where  $\lambda$  is the wavelength of the light source,  $a_2, b_2, c_2, d_2$  are the elements of the transfer matrix of path 2 or 3 and can be expressed as follows:

$$\begin{aligned} \begin{pmatrix} a_2 & b_2 \\ c_2 & d_2 \end{pmatrix} &= \begin{pmatrix} 1 & l_2 \\ 0 & 1 \end{pmatrix} \begin{pmatrix} 1 & 0 \\ -1/f & 1 \end{pmatrix} \begin{pmatrix} 1 & l_1 \\ 0 & 1 \end{pmatrix} \\ &= \begin{pmatrix} 1 - l_2/f & l_1 + l_2 - \frac{l_1 l_2}{f} \\ -1/f & 1 - l_1/f \end{pmatrix}. \end{aligned} \quad (9)$$

We assume the light source to be an incoherent light source with uniform intensity distribution  $I_0$ ; then its second-order correlation function at the source plane can be expressed as follows:

$$\langle E_s^*(x_1)E_s(x_2) \rangle = I_0 \delta(x_1 - x_2). \quad (10)$$

Substituting (6)–(9) into (2)–(5), after a tedious integration, we obtain

$$\langle I_1(u_1 = 0) \rangle \langle I_2(u_2) \rangle \langle I_3(u_3) \rangle \rightarrow \infty, \quad (11)$$

$$\Gamma_{12}(u_1 = 0, u_2)$$

$$\begin{aligned} &= \frac{I_0}{\sqrt{\lambda^2 f_1 f_e \sin \phi}} \int_{-\infty}^{\infty} H(v) \\ &\times \exp \left[ -\frac{i\pi}{\lambda f_e \tan \phi} (v^2 + u_2^2) + \frac{2i\pi}{\lambda f_e \sin \phi} vu_2 \right] dv, \end{aligned} \quad (12)$$

$$\Gamma_{13}(u_1 = 0, u_3)$$

$$= \frac{I_0}{\sqrt{\lambda^2 f_1 f_e \sin \phi}} \int_{-\infty}^{\infty} H(v) \times \exp \left[ -\frac{i\pi}{\lambda f_e \tan \phi} (v^2 + u_3^2) + \frac{2i\pi}{\lambda f_e \sin \phi} v u_3 \right] dv, \quad (13)$$

$$\Gamma_{23}(u_2, u_3) \rightarrow \infty. \quad (14)$$

In the above derivations, we have assumed the parameters of the optical system in Fig. 1 to be

$$l_1 = z + f_e \tan \frac{\phi}{2}, \quad l_2 = f_e \tan \frac{\phi}{2}, \quad f = f_e / \sin \phi. \quad (15)$$

Let's recall the definition of the conventional FRT, which is expressed as follows [24]

$$E_p(x_2) = \int_{-\infty}^{\infty} E_0(x_1) \exp \left[ -\frac{i\pi}{\lambda f_e \tan \phi} (x_1^2 + x_2^2) + \frac{i2\pi}{\lambda f_e \sin \phi} x_1 x_2 \right] dx_1, \quad (16)$$

where  $f_e$  is called “standard focal length”, and  $\phi$  is defined as  $p\pi/2$  with  $p$  being the fractional order of FRT. By comparing (12), (13) and (16), one finds that both (12) and (13) contain the FRT information of the object.

Now we discuss the properties of the sixth-order correlation  $G^{(3)}(u_1, u_2, u_3)$  (see (3)). The first term on the right side of (3) is the multiplication of the average intensity distribution at the three detectors, which does not contain FRT information of the object and acts as a background noise. The second term is the multiplication between the average intensity distribution at  $D_1$  and the square of the modulus of the second-order correlation between  $D_2$  and  $D_3$ , which also does not contain any FRT information of the object. The third term and the fourth term contain the FRT information of the object at  $D_2$  and  $D_3$  respectively. The fifth term is the multiplication of the second-order correlations between two arbitrary detectors, and the sixth term is the complex conjugate of the fifth term; they also contain the FRT information of the object.

Let us recall the fourth-order coincidence FRT with classical light, where the fourth-order correlation function between two detectors ( $D_1$  and  $D_2$  or  $D_1$  and  $D_3$ ) is expressed as follows [37, 38]:

$$G^{(2)}(u_1, u_2) = \langle I_1(u_1) \rangle \langle I_2(u_2) \rangle + |\Gamma_{12}(u_1, u_2)|^2. \quad (17)$$

One finds that only the second term of (17) contains the FRT information of the object. In the case of sixth-order coincidence FRT, there are four terms containing the FRT information of the object, which implies that the proportion of

the background noise in sixth-order coincidence FRT may be lower than that in fourth-order coincidence FRT, thus enhancing the visibility of the coincidence FRT pattern of the object. Equation (15) is a necessary condition for the optical system shown in Fig. 1 to implement the sixth-order coincidence FRT.

We note that the visibility of the sixth-order coincidence FRT pattern implemented with incoherent light is zero due to (11) and (14). To obtain visible sixth-order coincidence FRT pattern, we can replace the incoherent light source with a typical partially coherent light source, named the Gaussian Schell-model (GSM) source, whose second-order correlation function is expressed as [12–15]

$$\langle E_s^*(x_1) E_s(x_2) \rangle = \exp \left( -\frac{x_1^2 + x_2^2}{\sigma_{I0}^2} - \frac{(x_1 - x_2)^2}{\sigma_{g0}^2} \right), \quad (18)$$

where  $\sigma_{I0}$  and  $\sigma_{g0}$  are the transverse width and transverse coherence length of the GSM source, respectively. Similarly to fourth-order coincidence FRT [38], we can obtain the sixth-order coincidence FRT pattern of the object with good visibility and quality by choosing suitable values of  $\sigma_{I0}$ ,  $\sigma_{g0}$ .

### 3 Numerical results

In this section, we give some numerical results of the sixth-order coincidence FRT of an object implemented with partially coherent light. For the sake of comparison, the corresponding results of the fourth-order coincidence FRT of an object are also shown.

For the convenience of calculation, we assume  $u_2 = u_3$ , which means that  $D_2$  and  $D_3$  are placed in the same corresponding positions. In this case, we have

$$\begin{aligned} \Gamma_{31}(u_1 = 0, u_2) &= \Gamma_{12}^*(u_1 = 0, u_2), \\ \Gamma_{23}(u_2, u_2) &= \langle I_2(u_2) \rangle = \langle I_3(u_2) \rangle. \end{aligned} \quad (19)$$

The last two terms of  $G^{(3)}(u_1 = 0, u_2, u_2)$  is simplified as follows:

$$\begin{aligned} 2\text{Re}[\Gamma_{31}(u_1 = 0, u_2) \Gamma_{12}(u_1 = 0, u_2) \Gamma_{23}(u_2, u_2)] \\ = 2\langle I_2(u_2) \rangle |\Gamma_{12}(u_1 = 0, u_2)|^2. \end{aligned} \quad (20)$$

Then we rewrite the sixth-order correlation  $G^{(3)}(u_1 = 0, u_2, u_2)$  as follows:

$$\begin{aligned} G^{(3)}(u_1 = 0, u_2, u_2) &= 2\langle I_1(u_1 = 0) \rangle \langle I_2(u_2) \rangle^2 \\ &\quad + 4\langle I_2(u_2) \rangle |\Gamma_{12}(u_1 = 0, u_2)|^2. \end{aligned} \quad (21)$$

Substituting (6)–(9) and (18) into (4), (5) and (21), we can calculate the sixth-order coincidence FRT pattern of

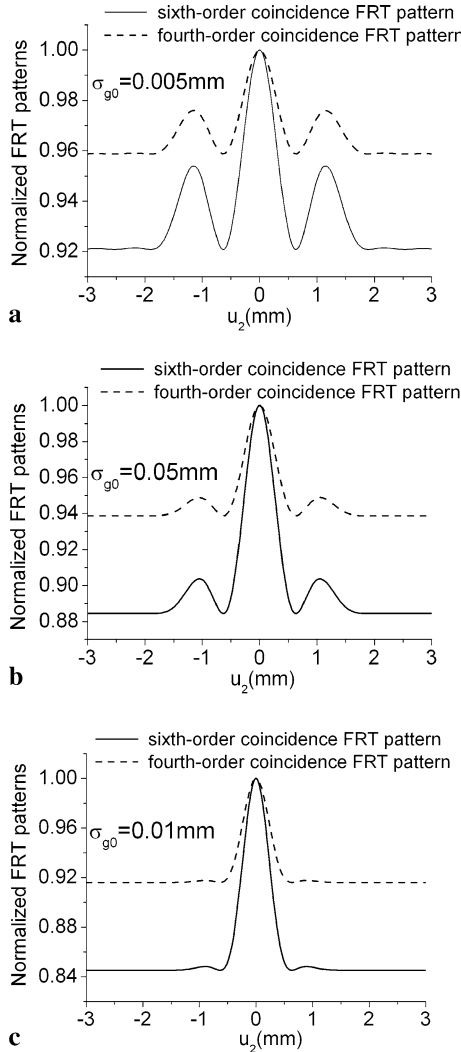


**Fig. 2** Normalized sixth-order coincidence FRT patterns (solid lines) of the double slit for different values of the transverse coherence length  $\sigma_{g0}$  of the GSM light source. The dotted lines correspond to the results of the fourth-order coincidence FRT patterns

an object implemented with a GSM light source numerically. We assume the object in our case to be a double slit whose transmission is  $H(v) = 1$  for  $-d/2 - a/2 < v < -d/2 + a/2$  and  $d/2 - a/2 < v < d/2 + a/2$ , and 0 for otherwise.  $a, d$  are slit width and the distance between two slits, respectively. We calculate in Fig. 2 the normalized sixth-order coincidence FRT patterns (solid lines)  $g^{(3)}(u_1 = 0, u_2, u_2)/g^{(3)}(u_1 = 0, u_2, u_2)_{\max}$  of the double slits for different values of the transverse coherence length  $\sigma_{g0}$  of the GSM light source with  $a = 100\text{ }\mu\text{m}$ ,  $d = 200\text{ }\mu\text{m}$ ,  $f_e = 40\text{ cm}$ ,  $\sigma_{I0} = 2\text{ mm}$ ,  $p = 1.0$ ,  $z = 15\text{ cm}$ ,  $\lambda = 632.8\text{ nm}$ . For comparison, the corresponding normalized fourth-order coincidence FRT patterns (dotted lines)  $g^{(2)}(u_1 = 0, u_2)/g^{(2)}(u_1 = 0, u_2)_{\max}$  of the double slits are also shown in Fig. 2. Here  $g^{(3)}(u_1 = 0, u_2, u_2)$  is defined as

follows:

$$g^{(3)}(u_1 = 0, u_2, u_2) = \frac{G^{(3)}(u_1 = 0, u_2, u_2)}{\langle \langle I_1(u_1 = 0) \rangle \langle I_2(u_2) \rangle \langle I_2(u_2) \rangle \rangle} \quad (22)$$

and  $g^{(2)}(u_1 = 0, u_2, u_2)$  is defined as follows

$$g^{(2)}(u_1 = 0, u_2) = \frac{G^{(2)}(u_1 = 0, u_2)}{\langle \langle I_1(u_1 = 0) \rangle \langle I_2(u_2) \rangle \rangle}. \quad (23)$$

One finds from Fig. 2 that we can obtain the visible FRT pattern of the double slit with good quality in both the sixth-order and fourth-order coincidence FRT cases when the source's transverse coherence length  $\sigma_{g0}$  is low (see Fig. 2(a)) and the source's transverse width  $\sigma_{I0}$  takes a finite value. As the transverse coherence length of the GSM source increases, the coincidence FRT pattern of the double slit gradually disappears (see Figs. 2(b)–(c)), but the visibility of the coincidence FRT pattern increases. In all cases, we find that the visibility of the sixth-order coincidence FRT pattern is much higher than that of the fourth-order coincidence FRT pattern. The visibility of the coincidence FRT pattern is defined as the maximum of the FRT pattern divided by the maximum of the coincidence counting rate. For the case of the sixth-order coincidence FRT, the visibility can be expressed as follows:

$$V = \frac{(4\langle I_2(u_2) \rangle |\Gamma_{12}(u_1 = 0, u_2)|^2)_{\max}}{G^{(3)}(u_1 = 0, u_2, u_2)_{\max}} \quad (24)$$

and for the case of fourth-order coincidence FRT, the visibility is expressed as follows:

$$V = \frac{|\Gamma_{12}(u_1, u_2)|^2_{\max}}{G^{(2)}(u_1, u_2)_{\max}}. \quad (25)$$

The visibilities are 0.0790, 0.115, 0.155 for Figs. 2(a)–(c) in the case of the sixth-order coincidence FRT patterns, and they are 0.0412, 0.0613, 0.0838 for Figs. 2(a)–(c) in the case of the fourth-order coincidence FRT patterns. Figure 3 shows the normalized sixth-order coincidence FRT patterns (solid lines) of the double slit for different values of the fractional order  $p$ . The corresponding normalized fourth-order coincidence FRT patterns (dotted lines) are also shown in Fig. 3. One finds from Figs. 3(a)–(f) that the visibility of the coincidence FRT pattern is also closely related to the fractional order  $p$ . As the value of  $p$  varies, the visibility changes. Our numerical results show that the dependence of the visibility on  $p$  is periodic with period 2. But for any value of  $p$ , the visibility of the sixth-order coincidence FRT pattern is much higher than that of the fourth-order coincidence FRT pattern.

Figure 4 shows the dependence of the visibility (solid line) of the sixth-order coincidence FRT pattern on the transverse coherence length with  $a = 100\text{ }\mu\text{m}$ ,  $d = 200\text{ }\mu\text{m}$ ,  $f_e =$

**Fig. 3** Normalized sixth-order coincidence FRT patterns (solid lines) of the double slit for different values of the fractional order  $p$ . The dotted lines correspond to the results of the fourth-order coincidence FRT patterns

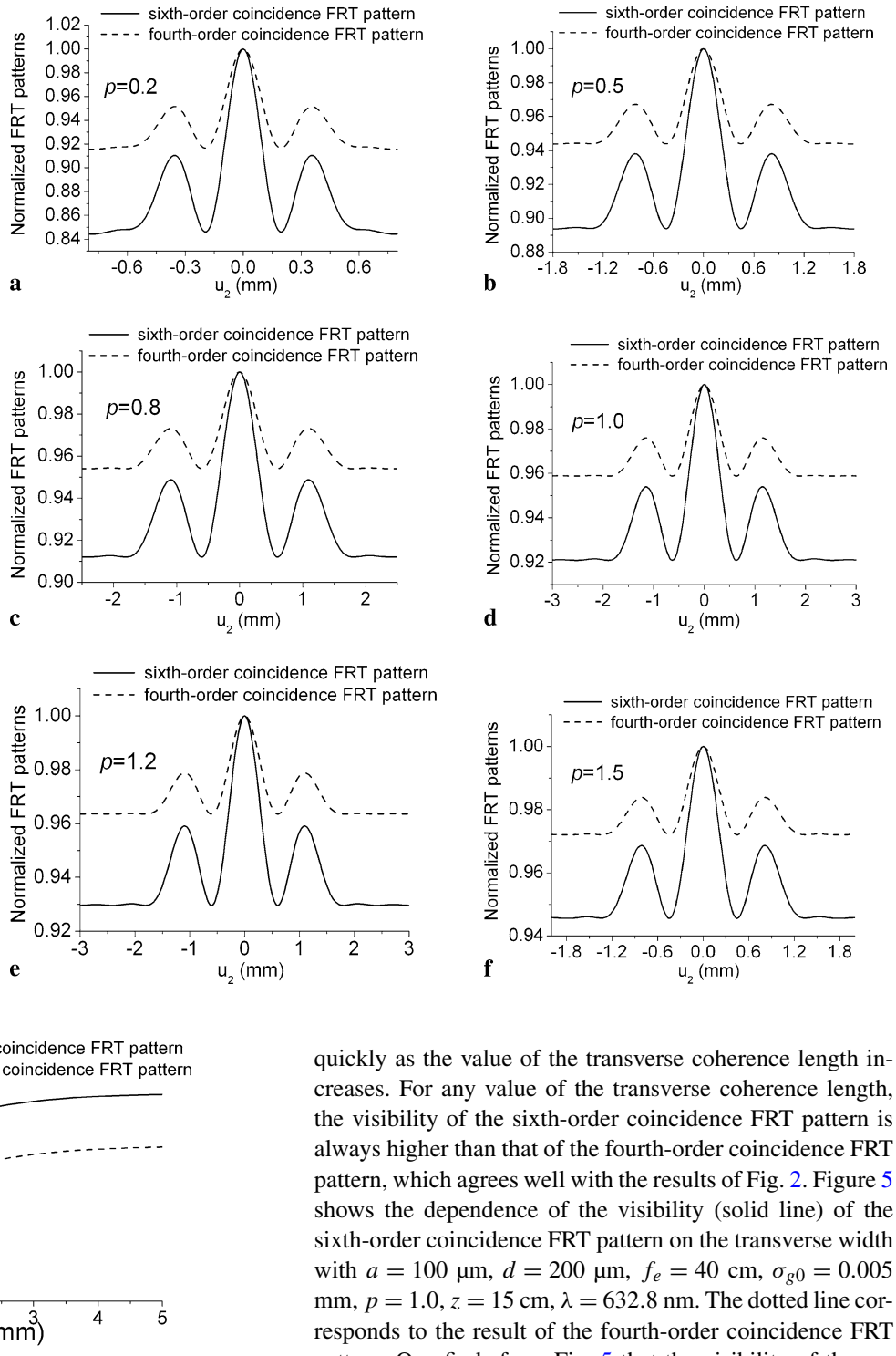


**Fig. 4** Dependence of the visibility (solid line) of the sixth-order coincidence FRT pattern on the transverse coherence length  $\sigma_{g0}$

$40 \text{ cm}$ ,  $\sigma_{I0} = 2 \text{ mm}$ ,  $p = 1.0$ ,  $z = 15 \text{ cm}$ ,  $\lambda = 632.8 \text{ nm}$ . The corresponding result of the fourth-order coincidence FRT pattern (dotted line) is also shown. It is clear from Fig. 3 that the visibility of the coincidence FRT pattern increases

quickly as the value of the transverse coherence length increases. For any value of the transverse coherence length, the visibility of the sixth-order coincidence FRT pattern is always higher than that of the fourth-order coincidence FRT pattern, which agrees well with the results of Fig. 2. Figure 5 shows the dependence of the visibility (solid line) of the sixth-order coincidence FRT pattern on the transverse width with  $a = 100 \mu\text{m}$ ,  $d = 200 \mu\text{m}$ ,  $f_e = 40 \text{ cm}$ ,  $\sigma_{g0} = 0.005 \text{ mm}$ ,  $p = 1.0$ ,  $z = 15 \text{ cm}$ ,  $\lambda = 632.8 \text{ nm}$ . The dotted line corresponds to the result of the fourth-order coincidence FRT pattern. One finds from Fig. 5 that the visibility of the coincidence FRT pattern decreases quickly as the transverse width increases, but the visibility of the sixth-order coincidence FRT pattern is always higher than that of the fourth-order coincidence FRT pattern for any value of the transverse width. From the above discussion, we can come to the conclusion that the sixth-order coincidence FRT indeed can enhance the visibility of the FRT pattern, while it is necessary for us to choose suitable values of  $\sigma_{I0}$  and  $\sigma_{g0}$ .

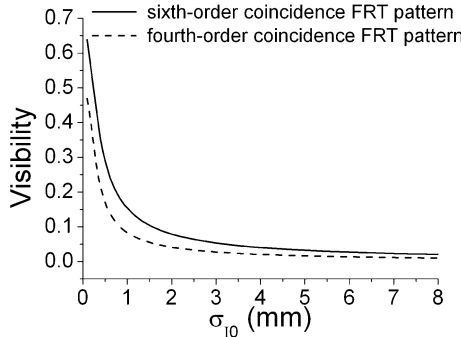


**Fig. 5** Dependence of the visibility (solid line) of the sixth-order coincidence FRT pattern on the transverse width  $\sigma_{10}$

#### 4 Summary

In conclusion, we have introduced the sixth-order coincidence FRT implemented with incoherent and partially coherent light, and we proposed an optical system to achieve the sixth-order coincidence FRT. The necessary condition for implementing the sixth-order coincidence FRT has been derived. Our numerical results show that the visibility of the sixth-order coincidence FRT pattern of an object is always much higher than that of the fourth-order coincidence FRT pattern, and its value is also closely related to the transverse width and the transverse coherence length of light source, and also depends on the fractional order of the optical system. Our method and results will enhance the application of the coincidence FRT. We expect to carry out the experiment in future to verify our results. Furthermore, in the present paper, we have adopted Lohmann's definition of the FRT, so the scale factors for the input and output planes are the same. For the more general case, the FRT can go with different scale factors for the input and output planes as shown in [56, 57]. We leave the coincidence FRFT with different scale factors for future study.

**Acknowledgement** Y. Cai acknowledges the support by the Foundation for the Author of National Excellent Doctoral Dissertation of P.R. China under Grant NO. 200928.

#### References

1. E. Wolf, Phys. Rev. Lett. **56**, 1370 (1986)
2. E. Wolf, Nature **326**, 363 (1987)
3. L. Mandel, E. Wolf, *Optical Coherence and Quantum Optics* (Cambridge University Press, Cambridge, 1995)
4. J. Pu, H. Zhang, S. Nemoto, Opt. Commun. **162**, 57 (1999)
5. S. Anand, B.K. Yadav, H.C. Kandpal, J. Opt. Soc. Am. A **19**, 2223 (2002)
6. J.C. Ricklin, F.M. Davidson, J. Opt. Soc. Am. A **19**, 1794 (2002)
7. M.S. Zubairy, J.K. McIver, Phys. Rev. A **36**, 202 (1987)
8. Y. Cai, U. Peschel, Opt. Express **15**, 15480 (2007)
9. Y. Kato, K. Mima, N. Miyanaga, S. Arinaga, Y. Kitagawa, M. Nakatsuka, C. Yamanaka, Phys. Rev. Lett. **53**, 1057 (1984)
10. A. Belendez, L. Carretero, A. Fimia, Opt. Commun. **98**, 236 (1993)
11. G.C. Dente, J.S. Osgood, Optim. Eng. **22**, 720 (1983)
12. E. Collett, E. Wolf, Opt. Lett. **2**, 27 (1978)
13. F. Gori, Opt. Commun. **34**, 301 (1978)
14. Q. Lin, Y. Cai, Opt. Lett. **27**, 216 (2002)
15. P.D. Santis, F. Gori, G. Guattari, C. Palma, Opt. Commun. **29**, 256 (1979)
16. F. Wang, Y. Cai, J. Opt. Soc. Am. A **24**, 1937 (2007)
17. E. Tervonen, A.T. Friberg, J. Turunen, J. Opt. Soc. Am. A **9**, 796 (1992)
18. F. Gori, M. Santarsiero, G. Piquero, R. Borghi, A. Mondello, R. Simon, J. Opt. A Pure Appl. Opt. **3**, 1 (2001)
19. E. Wolf, Phys. Lett. A **312**, 263 (2003)
20. O. Korotkova, M. Salem, E. Wolf, Opt. Lett. **29**, 1173 (2004)
21. F. Gori, M. Santarsiero, R. Borghi, V. Ramírez-Sánchez, J. Opt. Soc. Am. A **25**, 1016 (2008)
22. V. Namias, J. Inst. Math. Appl. **25**, 241 (1973)
23. A.C. McBride, F.H. Kerr, IMA J. App. Math. **39**, 159 (1987)
24. A.W. Lohmann, J. Opt. Soc. Am. A **10**, 2181 (1993)
25. D. Mendlovic, H.M. Ozaktas, J. Opt. Soc. Am. A **10**, 1875 (1993)
26. H.M. Ozaktas, D. Mendlovic, J. Opt. Soc. Am. A **10**, 2522 (1993)
27. S.C. Pei, M.H. Yeh, T.L. Luo, IEEE Trans. Signal Process. **47**, 2883 (1999)
28. B. Zhu, S. Liu, Q. Ran, Opt. Lett. **25**, 1159 (2000)
29. X. Xue, H.Q. Wei, A.G. Kirk, Opt. Lett. **26**, 1746 (2001)
30. Y. Cai, Q. Lin, Opt. Commun. **217**, 7 (2003)
31. Q. Lin, Y. Cai, Opt. Lett. **27**, 1672–1674 (2002)
32. Y. Cai, Q. Lin, J. Opt. Soc. Am. A **20**, 1528 (2003)
33. Y. Cai, Q. Lin, J. Opt. A Pure Appl. Opt. **5**, 272 (2003)
34. Y. Cai, D. Ge, Q. Lin, J. Opt. A Pure Appl. Opt. **5**, 453 (2003)
35. Y. Cai, Q. Lin, J. Opt. A Pure Appl. Opt. **6**, 307 (2004)
36. F. Wang, Y. Cai, Q. Lin, J. Opt. Soc. Am. A **25**, 2001 (2008)
37. Y. Cai, Q. Lin, S. Zhu, Appl. Phys. Lett. **86**, 021112 (2005)
38. Y. Cai, S. Zhu, J. Opt. Soc. Am. A **22**, 1798 (2005)
39. T.B. Pittman, Y.H. Shih, D.V. Strekalov, A.V. Sergienko, Phys. Rev. A **52**, R3429 (1995)
40. D.V. Strekalov, A.V. Sergienko, D.N. Klyshko, Y.H. Shih, Phys. Rev. Lett. **74**, 3600 (1995)
41. A. Gatti, E. Brambilla, M. Bache, L.A. Lugiato, Phys. Rev. Lett. **93**, 093602 (2004)
42. J. Cheng, S. Han, Phys. Rev. Lett. **92**, 093903 (2004)
43. Y. Cai, S. Zhu, Opt. Lett. **29**, 2716–2718 (2004)
44. Y. Cai, S. Zhu, Phys. Rev. E **71**, 056607 (2005)
45. D. Cao, J. Xiong, K. Wang, Phys. Rev. A **71**, 013801 (2005)
46. F. Ferri, D. Magatti, A. Gatti, M. Bache, E. Brambilla, L.A. Lugiato, Phys. Rev. Lett. **94**, 183602 (2005)
47. A. Valencia, G. Scarcelli, M. D'Angelo, Y. Shih, Phys. Rev. Lett. **94**, 063601 (2005)
48. Y. Cai, Q. Lin, S. Zhu, J. Opt. Soc. Am. A **23**, 835 (2006)
49. Y. Cai, F. Wang, Opt. Lett. **31**, 2278 (2006)
50. F. Wang, Y. Cai, S. He, Opt. Express **14**, 6999 (2006)
51. L. Ou, L. Kuang, J. Phys. B At. Mol. Opt. Phys. **40**, 1833 (2007)
52. Y. Bai, S. Han, Phys. Rev. A **76**, 043828 (2007)
53. D. Cao, J. Xiong, S. Zhang, L. Lin, L. Cao, K. Wang, Appl. Phys. Lett. **92**, 201102 (2008)
54. H. Li, Y. Zhang, D. Cao, J. Xiong, K. Wang, Chin. Phys. B **17**, 1674 (2008)
55. A. Gerrard, J.M. Burch, *Introduction to Matrix Methods in Optics* (Wiley, New York, 1975)
56. P. Pellat-Finet, Opt. Lett. **19**, 1388 (1994)
57. S. Liu, J. Wu, C. Li, Opt. Lett. **20**, 1415 (1995)